arXiv:1209.0386v1 [physics.bio-ph] 3 Sep 2012

Self-similar dynamics of bacterial chemotaxis

Waipot Ngamsaad[1, *] and Kannika Khompurngson[2, 3]

[1] *Division of Physics, School of Science, University of Phayao, Mueang Phayao, Phayao 56000, Thailand*
[2] *Division of Mathematics, School of Science, University of Phayao, Mueang Phayao, Phayao 56000, Thailand*
[3] *Centre of Excellence in Mathematics, PERDO, CHE, Thailand*

(Dated: September 4, 2012)

We investigate the pattern formation of colony generated by chemotactic bacteria through a continuum model. In a simplified case, the dynamics of system is governed by a density-dependent convection-reaction-diffusion equation, $u_t = (u^m)_{xx} - 2\kappa(u^m)_x + u - u^m$. This equation admits the analytical solutions that show the self-similarity of the bacterial colony's morphogenesis. In addition, we found that the colony evolves long time as the sharp traveling wave. The roles of chemotaxis on the regulation of pattern formation in these results are also discussed.

PACS numbers: 87.18.Hf, 05.45.-a, 87.23.Cc, 82.40.Ck

The spatiotemporal pattern formation in bacterial colony is an example of elegant self-organization in nature. This phenomenon attracts much attentions of scientist in interdisciplinary fields for decades [1, 2]. The pattern formations are not only resulted from reproduction and movement in bacterial populations but also from the cooperation of the individual to cope with the hostile environmental conditions. This collective behavior reflects the bacterial communication capabilities and social intelligence which might promise the new paradigm for biocomplexity and natural computations [3, 4]. The underlying mechanism of bacterial pattern formation is a key to understand living organisms, which is therefore important to biotechnology and medical science.

It has demonstrated that the colony of various bacterial species exhibits branching pattern [1, 5–7] which is analogous to the fractal pattern formation in the diffusion-limited aggregation (DLA) process [8]. In this manner, the bacterial colony's patterns are typically self-similar, where they are the same at every scale (scale invariant). This macroscopic pattern is arisen from the microscopic behavior of each individual member of bacteria in colony. The bacteria move in fluid medium by swimming as random walk motion, in which the bacteria propel themselves in nearly straight run separated by brief tumble. Unlike nonliving particles, the bacteria respond to a chemical attractant such as nutrient by swimming along its gradient, known as the chemotaxis. The chemotaxis has an essential role on the regulation of bacterial colony pattern formation as demonstrated by Refs. [9–11]. The bacteria detect the spatial gradients by comparing a temporal difference between the amount of attractant molecules that bind to the membrane receptors along their path. The bacteria implement the chemotaxis by delaying the tumbling frequency as cells swim up the gradient of the attractant or down the gradient of repellent. Moreover, the bacteria perform the intricate cellular communications capacities in forming the colony to respond the environmental conditions: These includes long range chemical signaling, such as quorum sensing and chemotactic signaling. At first glance, the formation of bacterial colonies appears quite complicated; but the reaction-diffusion model has successfully described the continuum limit of this dynamics [1, 2, 6, 7].

In this Letter, we consider a nonlinear reaction-diffusion model that has been proposed for studying the pattern formation in bacterial colonies exemplified by *Paenibacillus dendritiformis* grown on Petri dish [1, 7, 12, 13]. This bacteria species is motile on the dry surface by cooperatively producing a layer of lubrication fluid in which they swim and its colony exhibits branching pattern. Indeed, the numerical simulations on this model has been carried out from past studies [7, 12, 13]. It seems likely that the numerical results reproduce the branching pattern in the bacterial colonies, which agrees well in comparison with experimental data. However, the sole numerical results are inadequate to explain the scaling laws of bacterial colony growth. Thus, an analytical result is still required to archive this task. The aim of this work is to analyze the simplified form of those proposed nonlinear reaction-diffusion models for pattern formation in bacterial colony, which takes chemotaxis into account [1, 7, 12, 13]. Our analytical results could be plausible for interpreting the results in both experiments and simulations.

We now explain the bacterial chemotaxis model in our consideration. Actually, the bacterial colony evolves in two dimensions however; each tip grows in one dimension, except for occasional branching. Thus, it allows us to investigate this problem in one-dimensional space which its results could be equivalent to one obtained from the two-dimensional system [6]. As proposed in Ref. [14], the dynamics of bacterial populations is governed by a generalized convection-reaction-diffusion (CRD) equation

$$\frac{\partial u}{\partial t} = \frac{\partial}{\partial x}\left(D(u)\frac{\partial u}{\partial x} - u\vartheta(s)\right) + R(u), \qquad (1)$$

where $u(x, t)$ and $s(x, t)$ are, respectively, the bacterial density and the attractant density in spatial coordinate x and time t. $D(u)$, $R(u)$ and $\vartheta(s)$ are, respectively, the diffusion coefficient, the reaction term and the drift velocity due to the chemotaxis. This equation is similar to the generalized Keller-Segel equation [15]. Eq. (1) is a simplified form of the full model in Refs. [7, 12, 13] under following assumptions. i) The nutrient density is proportional to the bacterial density and is absorbed some way in reaction term. ii) The production of lubricant fluid is proportional to the bacterial density and is absorbed into the medium. Thus, the lubrication fluid can be removed from the dynamics and it is represented through the diffusion coefficient [12, 14]. iii) The chemotactic signal can be also a field produced directly or indirectly by the bacterial cells.

In the usual case, the diffusion coefficient is constant which represents the Brownian motion or random walk. Since the random walk seems to be unrealistic movement for the active individual such as members of biological population, the crowd-avoidance movement has been introduced [16–20]. In this case, the diffusion coefficient is represented by a density-dependent form $D(u) = M(u/\sigma)^p$, where $M > 0$ is diffusion constant, $\sigma = \lim_{t\to\infty} u(x,t)$ is equilibrium density and $p > 0$. For the reaction term, it can be represented by the generalized logistic law $R(u) = \alpha u[1 - (u/\sigma)^p]$, where $\alpha > 0$ is rate constant [20]. The chemotatic drift velocity can be expressed as $\vartheta(s) = \zeta(s)\chi(s)s_x$, where $\chi(s)s_x$ acts as the gradient sensed by the bacterium (with $\chi(s)$ having the units of 1 over the chemical concentration) [12]. $\zeta(s)$ is the bacterial response to the sensed gradient and has the same units as a diffusion coefficient [12]. Therefore, we assume $\zeta(s) = \gamma D(u) = \gamma M(u/\sigma)^p$ where γ is a constant, positive for attractive chemotaxis and negative for repulsive chemotaxis [12]. Here, we are interest in a special case where the gradient sensed by the bacterium is nearly uniform and $\chi(s)s_x$ is treated as a constant [14].

By substituting $D(u)$, $R(u)$ and $\vartheta(s)$ into Eq. (1) with the transformations $t^* = \alpha t$, $x^* = (m\alpha/M)^{\frac{1}{2}}x$, $u^* = u/\sigma$ and $\kappa = (1/2)\gamma(mM/\alpha)^{\frac{1}{2}}\chi(s)s_x$, we obtain the dimensionless equation

$$u_t = (u^m)_{xx} - 2\kappa(u^m)_x + u - u^m, \tag{2}$$

where $m = p + 1 > 1$ and the asterisk is dropped. The traveling wave *ansatz* to Eq. (2) has been analyzed [14, 21]. It found that there exists traveling wave solution for wave speeds equal to or greater than the minimum value [14, 21]. Although the solution of Eq. (2) has well understood as the traveling wave, the exact or explicit solution in space-time coordinate has been unknown. In addition, it has been pointed that the traveling wave solution is only intermediate asymptotic behavior of system [22]. Therefore, it is still unclear that how the systems evolve to traveling wave from an initial state. In previous study by Ref. [23], Eq. (2) can be mapped to an inhomogeneous diffusion equation by a transformation technique, where the reaction term is eliminated. However, the exact solution has not been obtained in the closed-form. In our previous work [24], Eq. (2) without chemotaxis can be differently mapped to an anomalous diffusion equation [25–27] which the exact self-similar solution can be obtained for any $m > 2$. We then extend the similar technique to analyze Eq. (2).

We perform the analysis on Eq. (2) with similar method to Refs. [23, 24]. Note that Eq. (2) can be written in equivalent form as

$$\left(\frac{\partial}{\partial t} - 1\right)u = \frac{1}{\omega^2}\left(\frac{\partial}{\partial y} + 1\right)\left(\frac{\partial}{\partial y} - \omega^2\right)u^m, \tag{3}$$

where $y = x/\omega$ and $\omega = \kappa \pm \sqrt{\kappa^2+1}$. Next, Eq. (3) can be evaluated to $e^t\frac{\partial}{\partial t}e^{-t}u = \omega^{-2}e^{-y}\frac{\partial}{\partial y}e^y(e^{\omega^2 y}\frac{\partial}{\partial y}e^{-\omega^2 y}u^m)$. To eliminate the exponential terms in Eq. (3), we define the solution as

$$u(y,t) = e^t e^{\frac{\omega^2}{m}y}\Phi(y,t). \tag{4}$$

By substituting Eq. (4) into Eq. (3), we obtain $e^{-(m-1)t}\Phi_t = \omega^{-2}e^{-\frac{(m+\omega^2)}{m}y}[e^{(\omega^2+1)y}(\Phi^m)_y]_y$. By introducing the variable transforms $d\tau = (m-1)e^{(m-1)t}dt$ and $d\phi = \frac{m+\omega^2}{m}e^{(m+\omega^2)y/m}dy$ that gives

$$\begin{aligned}\tau(t) &= e^{(m-1)t} - 1 \\ \phi(y) &= e^{\frac{(m+\omega^2)}{m}y},\end{aligned} \tag{5}$$

this equation can be reduced further to

$$\Phi_\tau = k[\phi^l(\Phi^m)_\phi]_\phi, \tag{6}$$

where $k = \frac{1}{\omega^2(m-1)}\left(\frac{m+\omega^2}{m}\right)^2$ and $l = \frac{(\omega^2+2)m+\omega^2}{m+\omega^2}$. Eq. (6) has the form of anomalous diffusion equation as studied in Refs. [25–27]. To obtain the solution of Eq. (6), we assume the solution to be the scaling function of the type

$$\Phi(\phi,\tau) = \frac{1}{T(\tau)}F\left(\frac{\phi}{T(\tau)}\right) = \frac{F(\theta)}{T(\tau)}, \tag{7}$$

where $\theta(\phi,\tau) = \phi/T(\tau)$ [24–27]. By substituting Eq. (7) into Eq. (6), we obtain $-\frac{T_\tau}{T^2}(F + \theta F_\theta) = \frac{k}{T^{m-l+2}}\left[\theta^l(F^m)_\theta\right]_\theta$ which can be separated into two equations: $T^{m-l}T_\tau = \lambda$ and $-\lambda(\theta F)_\theta = k\left[\theta^l(F^m)_\theta\right]_\theta$ where λ is constant. Performing calculations similar to Refs. [24–27] and choosing $\lambda = (m-l+1)^{-1}$, we obtain

$$\begin{aligned}T(\tau) &= (\tau + a)^{\frac{m+\omega^2}{m(m-1)}} \\ F(\theta) &= \left[b + \theta^{\frac{-(m-1)\omega^2}{m+\omega^2}}\right]^{\frac{1}{m-1}},\end{aligned} \tag{8}$$

where $a > 0$ and b are constant. By substituting Eq. (8) back into the main solution Eq. (4), after doing some algebra, we obtain the explicit solution to Eq. (2)

$$u(x,t) = \frac{e^t}{(e^{pt}-1+a)^{\frac{1}{p}}}\left\{1 + b\left[\frac{e^{p\omega x}}{(e^{pt}-1+a)^{\omega^2}}\right]^{\frac{1}{p+1}}\right\}^{\frac{1}{p}}. \tag{9}$$

We now consider the initial condition for solution (9) $u_0(x) = u(x,0)$ that has *(semi-)*compact support: $\lim_{x\to-\infty} u_0(x) = \rho$ and $u_0(x) = 0$ for $x \geqslant x_0$, where ρ is initial density amplitude and x_0 is initial front position. Such conditions, we obtain $a = \rho^{-p}$ and $b = -\rho^{-p\omega^2/(p+1)}e^{-p\omega x_0/(p+1)}$. By substituting the constant a and b into Eq. (9), we obtain the exact solution to Eq. (2)

$$u(x,t) = \frac{\rho e^t}{[\rho^p(e^{pt}-1)+1]^{\frac{1}{p}}} \times \left\{1 - \left[\frac{e^{p\omega(x-x_0)}}{[\rho^p(e^{pt}-1)+1]^{\omega^2}}\right]^{\frac{1}{p+1}}\right\}^{\frac{1}{p}}. \qquad (10)$$

Since the solution Eq. (10) has two forms depending on the value of ω, we define $u_+(x,t)$ and $u_-(x,t)$ are the solutions corresponding to $\omega_+ = \kappa + \sqrt{\kappa^2+1}$ and $\omega_- = \kappa - \sqrt{\kappa^2+1}$, respectively. We now construct another solution of Eq. (2) by linear combination of these two solutions:

$$w(x,t) = u_+(x,t) + u_-(x,t). \qquad (11)$$

By using binomial expansion, we obtain an approximation

$$w^m = (u_+ + u_-)^m \approx u_+^m + u_-^m + \mathcal{O}(H), \qquad (12)$$

where $H = \sum_{k=1}^{m-1}\binom{m}{k}u_+^k u_-^{m-k}$. By substituting Eq. (11) as solution into Eq. (2) and using Eq. (12), we obtain $w_t = (w^m)_{xx} - 2\nu(w^m)_x + w - w^m + \mathcal{O}(H_{xx} - 2\nu H_x - H)$. Therefore, $w(x,t)$ in Eq. (11) can be a solution of Eq. (2) if the correction $\mathcal{O}(H_{xx} - 2\nu H_x - H)$ can be ignored. Using Eq. (12), we obtain the solution

$$w(x,t) \approx 2^{-\frac{1}{p}}\left[u_+^p(x,t) + u_-^p(x,t)\right]^{\frac{1}{p}}, \qquad (13)$$

where $(2)^{-1/p}$ is normalized factor. We note that in case of no chemotaxis $\kappa = 0$, thus $\omega = \pm 1$, these results have been discussed in our previous work [24].

The evolution in space and time of bacterial density profile $u_+(x,t)$ and $u_-(x,t)$, as in Eq. (10), are illustrated in Fig. (1). It is seen that the density profiles start from the initial state $u_0(x)$ then grow and expand to the unoccupied region. At sufficient large time scale, the density profiles reach the saturated point with the maximum value 1. After that, they seem to propagate with unchanged shape; $u_+(x,t)$ is propagating to the right whereas $u_-(x,t)$ is propagating to the left. Roles of chemotaxis on the regulation of pattern formation in the system is reflected by parameter κ. Since $\kappa < \sqrt{\kappa^2+1}$, ω_+ is always positive whereas ω_- is always negative that leads the tails of u_+ to decay as $x \to \infty$ and the tails of u_- decay as $x \to -\infty$. In the former case, the front-interface is sharper because $|\omega_+| > |\omega_-|$. Due to the influence of chemotaxis, the distribution of density profile is biased toward to the right thus the front of u_+ is moving faster than of u_-. The spatiotemporal evolution of the combined density profiles $w(x,t)$ is also illustrated in Fig. (2). The density $w(x,t)$ form the pulse-like profile that grow and expand with asymmetric shape. It behaves like $u_+(x,t)$ for $x \gg x_0$ and behaves like $u_-(x,t)$ for $x \ll -x_0$. Due to the bias force from chemotaxis, the peak of $w(x,t)$ is moving toward to the right.

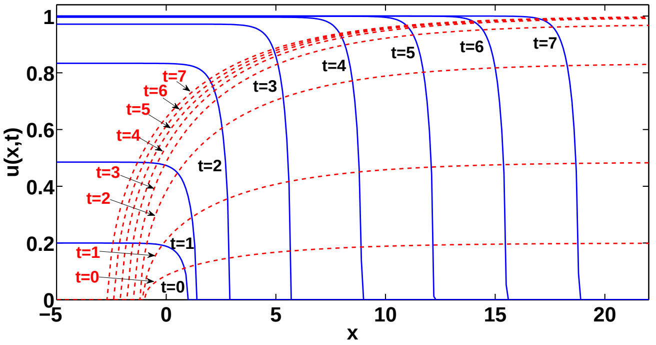

FIG. 1. The spatiotemporal evolution of the density profile $u(x,t)$ (Eq. (10)) in the case of $p = 2$ with initial conditions $\rho = 0.2$ and $x_0 = 1$. The solid lines represent $u_+(x,t)$ and the dashed lines represent $u_-(x,t)$.

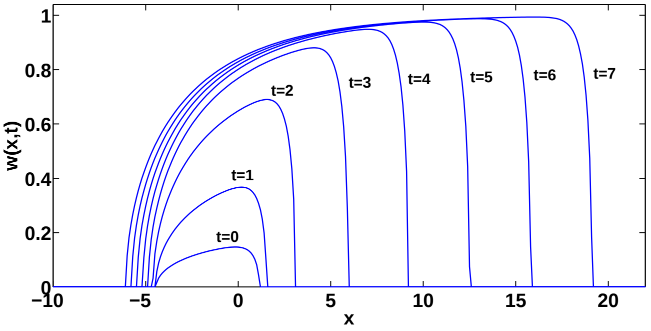

FIG. 2. The spatiotemporal evolution of the pulse-like density profile $w(x,t)$ (Eq. (13)) in the case of $p = 2$ with initial conditions $\rho = 0.2$ and $x_0 = 1$.

From Eq. (10), we calculate the front position $r(t)$, that the density falls to zero $u(r,t) = 0$ as $r(t) = x_0 + \omega\frac{\ln[\rho^p(e^{pt}-1)+1]}{p}$. The plot of relative front position $r(t) - x_0$ is shown in Fig. (3). The relative front position of $u_-(x,t)$ is slow varying when compared with of $u_+(x,t)$. At sufficient large time, that $e^{pt'} \gg 1$ and $\rho^p e^{pt'} \gg 1$ thus $t' \approx -\ln\rho$, the relative front position seems to vary linearly in time $r(t) - x_0 \sim \omega t$. It implies the constant front propagating speed. Consequently, we calculate the front speed as $v(t) = \frac{d}{dt}r(t) = \frac{\omega\rho^p e^{pt}}{\rho^p(e^{pt}-1)+1}$. At large time scale $t \gg t'$, the spreading speed trends to be the constant $c = \lim_{t\to\infty} v(t) = \omega(\kappa)$. At this point, it is clearly seen that the spreading speed is biased by the chemotaxis through the parameter κ.

At the large time scale, $t \gg t'$, the bacterial density

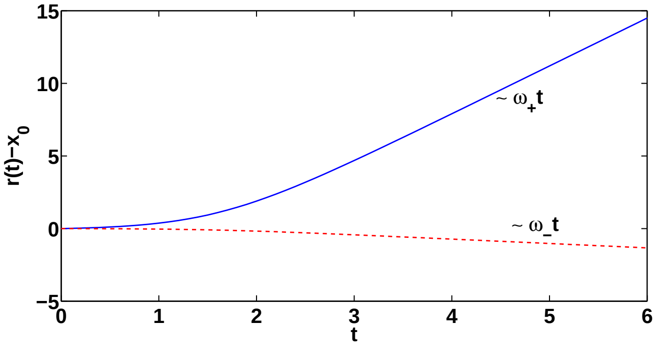

FIG. 3. The relative front position $r(t)-x_0$ corresponding to density profile in Fig. (1). The solid lines represent the relative front position of $u_+(x,t)$ and the dashed lines represent the relative front position of $u_-(x,t)$.

profile Eq. (10) emerges the traveling wave form

$$\widetilde{u}(x-\omega t)=\left[1-\frac{e^{\frac{p\omega}{p+1}(x-\omega t-x_0)}}{\rho^{\frac{p\omega^2}{p+1}}}\right]^{\frac{1}{p}}, \tag{14}$$

where ω is front speed. When converting to the physical dimension, the front speed obtained here is comparable to the minimum value $c_{min}=\omega\sqrt{\frac{M\alpha}{p+1}}$ for the sharp traveling wave front [14, 21]. Similarly, at the large time scale $t\gg t'$, Eq. (13) develops to the expanding pulse-like wave

$$\widetilde{w}(x-\omega_\pm t)\approx 2^{-\frac{1}{p}}\left[\widetilde{u}_+^p(x-\omega_+ t)+\widetilde{u}_-^p(x-\omega_- t)\right]^{\frac{1}{p}}, \tag{15}$$

with the expanding speed $\omega_\pm$.

We point out that, at large time scale $t\gg t'$, the solution Eq. (7) forms a scaling law $\Phi(\phi,\tau)\approx\frac{1}{\tau^\beta}F(\frac{\phi}{\tau^\beta})$, where $\beta=\frac{m+\omega^2}{m(m-1)}$. In biological context, the solution captures the self-similar features of the spatiotemporal pattern formation in bacterial colonies in the terms of transformed quantities: $u\rightarrow e^{\omega x/m}e^t\Phi$, $\tau\rightarrow e^{(m-1)t}$, and $\phi\rightarrow e^{(m+\omega^2)(x-x_0)/m\omega}$. This self-similar solution converges to the traveling wave solution which its behavior can be classified as the intermediated asymptotics of the second type, as described in Ref. [22].

In summary, we investigated the spatiotemporal pattern formation of bacterial chemotaxis described by a density-dependent convection-reaction-diffusion equation. The analytical solutions are obtained for the simplified case, where the gradient sensed by the bacterium is nearly uniform. The solutions show explicitly the self-similar structure of the bacterial colony growth. Consequently, the scaling law of bacterial colony growth is reveled. As usual, the solutions evolve long time scale as the traveling wave.

K. Khompurngson acknowledges the Centre of Excellence in Mathematics (Thailand) for partial financial support.

---

[*] waipot.ng@up.ac.th

[1] E. Ben-Jacob, I. Cohen, and H. Levine, Adv. Phys. **49**, 395 (2000).
[2] J. Murray, *Mathematical Biology I: An Introduction* (Springer, New York, 2002).
[3] E. Ben-Jacob, I. Becker, Y. Shapira, and H. Levine, Trends Microbiol. **12**, 366 (2004).
[4] E. Ben-Jacob, Ann. NY. Acad. Sci. **1178**, 78 (2009).
[5] T. Matsuyama and M. Matsushita, Appl. Environ. Microbiol. **58**, 1227 (1992).
[6] K. Kawasaki, A. Mochizuki, M. Matsushita, T. Umeda, and N. Shigesada, J. Theor. Biol. **188**, 177 (1997).
[7] I. Golding, Y. Kozlovsky, I. Cohen, and E. Ben-Jacob, Physica A **260**, 510 (1998).
[8] T. A. Witten and L. M. Sander, Phys. Rev. Lett. **47**, 1400 (1981).
[9] J. Adler, Science **153**, 708 (1966).
[10] E. Budrene and H. Berg, Nature **349**, 630 (1991).
[11] E. Budrene and H. Berg, Nature **376**, 49 (1995).
[12] I. Cohen, I. Golding, Y. Kozlovsky, E. Ben-Jacob, and I. Ron, Fractals **7**, 235 (1999).
[13] Y. Kozlovsky, I. Cohen, I. Golding, and E. Ben-Jacob, Phys. Rev. E **59**, 7025 (1999).
[14] B. Gilding and R. Kersner, J. Phys. A: Math. Gen. **38**, 3367 (2005).
[15] M. Tindall, P. Maini, S. Porter, and J. Armitage, Bull. Math. Biol. **70**, 1570 (2008).
[16] W. Gurney and R. Nisbet, J. Theor. Biol. **52**, 441 (1975).
[17] W. Gurney and R. Nisbet, J. Theor. Biol. **56**, 249 (1976).
[18] M. Gurtin and R. MacCamy, Math. Biosci. **33**, 35 (1977).
[19] W. Newman, J. Theor. Biol. **85**, 325 (1980).
[20] W. Newman, J. Theor. Biol. **104**, 473 (1983).
[21] M. Mansour, Rep. Math. Phys. **66**, 375 (2010).
[22] G. Barenblatt and Y. Zel'dovich, Annu. Rev. Fluid Mech. **4**, 285 (1972).
[23] P. Rosenau, Phys. Rev. Lett. **88**, 194501 (2002).
[24] W. Ngamsaad and K. Khompurngson, Phys. Rev. E **85**, 066120 (2012).
[25] M. Bologna, C. Tsallis, and P. Grigolini, Phys. Rev. E **62**, 2213 (2000).
[26] C. Tsallis and E. Lenzi, Chem. Phys. **284**, 341 (2002).
[27] E. Lenzi, L. Malacarne, R. Mendes, and I. Pedron, Physica A **319**, 245 (2003).